

Promotion of Binary Nitride Catalysts: Isothermal N₂ Adsorption, Microkinetic Model, and Catalytic Ammonia Synthesis Activity

Astrid Boisen, Søren Dahl, and Claus J. H. Jacobsen¹

Haldor Topsøe A/S, Nymøllevej 55, DK-2800 Lyngby, Denmark

Received October 25, 2001; revised February 13, 2002; accepted February 13, 2002

The kinetics of ammonia synthesis and N₂ dissociation over cesium-promoted Co₃Mo₃N are studied. The results support recent DFT calculations and explain why Co₃Mo₃N shows a higher ammonia synthesis activity than either constituting metal. The ammonia synthesis activity of cesium-promoted Co₃Mo₃N is reported for a series of conditions, with H₂:N₂ ratios of both 3:1 and 1:1, total pressures of 50, 25, and 10 bar, and temperatures from 593 to 713 K. Isothermal N₂ adsorption experiments were carried out and the results were well described by a simple model. The total number of surface sites on the catalyst capable of binding nitrogen was found to be approximately 30 μmol/g of catalyst. When only 1% of these surface sites is active for N₂ dissociation, the initial sticking coefficient, *s*₀, of dinitrogen on the active sites was found to be $s_0 = 0.1727 \cdot \exp(-42.8 \pm 5 \text{ kJ/mol}/RT)$. This result was used as input to a microkinetic model for ammonia synthesis where it was assumed that N* and H* are the only surface intermediates. In this way it was possible to obtain a good fit to the ammonia synthesis activity data with the nitrogen-binding energy as the only adjustable parameter. © 2002 Elsevier Science (USA)

Key Words: ammonia synthesis; microkinetic analysis; dinitrogen adsorption; promotion; nitride catalyst.

INTRODUCTION

During the last decades, there has been a continuous interest in heterogeneous carbide and nitride catalysts (1). Focus has primarily been on binary nitrides and carbides of molybdenum and tungsten (e.g., Mo₂N, W₂C, MoN, and WC) since these materials were claimed to possess platinumlike properties as catalysts in a number of processes (2, 3). Furthermore, these nitrides and carbides are easily prepared with very high surface areas (>50 m²/g) by ammonolysis or carburization of oxide precursors (4, 5). Since the resulting catalysts have high densities, high surface areas per reactor volume can be realized, which is of importance in many industrial applications. Nitride and carbide catalysts have been reported to have higher activities than currently used industrial catalysts in a substantial number of applications and therefore it is conspicuous that none

has been commercialized, so far. Particularly binary nitride and carbide catalysts have been reported to exhibit high activities in hydroprocessing reactions (6–8), steam-reforming (9, 10), water–gas shift (11), ammonia synthesis (12), isomerization (13), hydrogenation/dehydrogenation (14, 15), and hydrogenolysis (16). It appears however that for some of the above reactions, the nitride or carbide catalysts are unstable under industrially relevant conditions, as was recently shown for the steam-reforming reaction (17). Furthermore, it appears that in several cases the reported catalytic activities are not as promising as initially suggested. In some instances, the catalysts are compared on a turnover frequency basis and the high turnover frequencies result from very few active sites on the nitride or carbide catalyst even though they have very high surface areas. In other cases, the nitride or carbide catalysts are compared with industrial catalysts that for some reason (such as poor activation procedures) exhibit significantly lower activities than are found in commercial operation. Nevertheless, new possibilities might arise from the use of nitride and carbide catalysts. This could be in new reactions that are only effectively catalyzed by such materials. An example is the dehydrocyclization of methane to form benzene over molybdenum carbide on HZSM-5 catalysts (18). This reaction is one of the rare examples of a single-step gas-to-liquid process. It has been shown that the lifetime of this catalyst, which is usually shorter than 48 h and thus remains a key obstacle, can be improved by a carefully controlled activation procedure that influences the molybdenum carbide phase formed (19). Alternatively, nitride and carbide catalysts can be improved by promotion. Recently, there has been increasing interest in promotion of molybdenum and tungsten nitride and carbide catalysts with iron, cobalt, and nickel (20–26). Particularly for ammonia synthesis, such a promoted nitride catalyst, Cs/Co₃Mo₃N, has recently been shown to have a stable activity that is significantly higher than that of the commercial multipromoted iron catalyst (20, 21). Cs/Ni₂Mo₃N was also found to exhibit a high catalytic activity in ammonia synthesis (21). Kojima and Aika later independently verified the high activity of Cs/Co₃Mo₃N (22–24). However, this promoted ternary nitride catalyst is significantly more

¹ To whom correspondence should be addressed. Fax: +45 45 27 29 99. E-mail: asb@topsoe.dk.

expensive than the conventional iron catalyst and this has to be counterbalanced by similar cost savings for the catalyst to achieve any commercial potential. Although the catalytic ammonia synthesis reaction can be considered one of the currently best understood heterogeneously catalyzed reactions (27), it is not clear why Cs/Co₃Mo₃N is such an efficient catalyst. Recently, it was shown that the ammonia synthesis activity of both unpromoted (28) and promoted (29) catalysts is essentially governed by the nitrogen-binding energy. The explanation for this is that the activation energy for N₂ dissociation—the rate-limiting step—closely follows the nitrogen-binding energy, which is in agreement with the so-called Brønsted–Evans–Polanyi relationship. Thus, the requirement of both high activity and low surface intermediate stability results in a volcano curve when the ammonia synthesis activity is plotted as a function of the nitrogen-binding energy. Compared to the best catalysts Mo has too high and Co too low a nitrogen-binding energy to be efficient ammonia synthesis catalysts. It was shown by density functional theory (DFT) calculations that the nitrogen-binding energy of a CoMo alloy is intermediate between that of cobalt and molybdenum and consequently closer to the optimal binding energy (30). It was suggested that this interpolation concept is not limited to ammonia synthesis catalysts. We decided to study the kinetics of ammonia synthesis and N₂ dissociation over Cs/Co₃Mo₃N to further elucidate the potential of ternary nitrides as ammonia synthesis catalysts. A more complete understanding of these catalysts might also provide new insight into the effects of promoting carbides and nitrides and thereby guide further studies on such catalysts.

METHODS

The ternary nitride Co₃Mo₃N is prepared as previously described by ammonolysis of the solid oxide precursor CoMoO₄ · xH₂O. The oxide precursor is obtained by mixing a solution of cobalt(II) nitrate with a solution of ammonium heptamolybdate in equimolar amounts (Co/Mo = 1). The mixture is evaporated to dryness and calcined at 873 K for 5 h. The resulting CoMoO₄ · xH₂O is heated in a stream of 4.5% NH₃ in 3 : 1 H₂ : N₂ at 6.0 K/h to 873 K and kept at this temperature for 24 h. After cooling to room temperature, it is confirmed by X-ray powder diffraction (XRPD) that pure Co₃Mo₃N with a crystal size of 215 Å [D(400)] is formed. The Co₃Mo₃N catalyst is promoted with 3.85% Cs by incipient wetness impregnation with an aqueous solution of cesium nitrate. The promoter content is determined by chemical analysis. Catalytic activity measurements, temperature-programmed desorption, and isothermal dinitrogen adsorption experiments are conducted using this catalyst, as described below. All results shown in the Results and Discussion section are obtained with this catalyst. Another Cs/Co₃Mo₃N catalyst is prepared by a completely

TABLE 1
Crystal Sizes and Surface Areas of Catalysts

Catalyst	Crystal size determined from XRPD (Å)	BET (m ² /g)
KM1	360	17.2
Cs/Co ₃ Mo ₃ N	215	23.3
Cs/Co ₃ Mo ₃ N (a)	520	8.5

analogous procedure using the same final temperature of 873 K. However, the heating ramp during nitridation is 120 K/h. XRPD shows only Co₃Mo₃N with a crystal size of 520 Å [D(400)]. This catalyst is promoted to contain 4.8% Cs. With this catalyst, referred to as Cs/Co₃Mo₃N (a), only catalytic activity measurements are performed. Table 1 gives surface areas and crystal sizes for the two ternary nitride catalysts studied and similar data are shown for the industrial multipromoted catalyst, KM1, for comparison. For activity measurements a glass-lined U-tube reactor is loaded with 0.3063 g of Cs/Co₃Mo₃N with particle sizes of 0.3–0.8 mm, giving a bed height of 12 mm. Total pressures of 50, 25, and 10 bar, temperatures in the range 593–713 K, and dihydrogen and dinitrogen flows of 2.4–16 L/h (STP) are used with H₂ : N₂ ratios of 3 and 1. Ammonia concentrations are measured by two nondispersive infrared detectors (BINOS, Leybold–Heraeus) operating in different concentration ranges which are calibrated weekly using reference gases. A similar series of activity measurements are performed analogously with Cs/Co₃Mo₃N (a). After passivation at room temperature for 24 h in 1000 ppm O₂ in N₂, the nitride catalysts contain about 4–5 wt% oxygen. However, the nitride catalysts are not stable in ambient air and eventually transform into oxides. Previous *in situ* X-ray powder diffraction studies (21) have shown that at ammonia synthesis conditions, the diffraction pattern can be attributed to pure Co₃Mo₃N. The entire set of activity measurements can be obtained from the authors.

Isothermal N₂ adsorption experiments are carried out, as previously reported for the multipromoted iron-based ammonia synthesis catalyst KM1R (31). A glass-lined U-tube reactor is loaded with 0.507 g of Cs/Co₃Mo₃N with particle sizes of 0.15–0.30 mm giving a bed height of 16 mm. The catalyst is reduced in a 3 : 1 mixture of dihydrogen and dinitrogen at 20 bar by increasing the temperature at 50 K/h to 823 K and is kept there for 14 h. Then the activity of the catalyst is measured at 673 K and compared to earlier measurements. Between the individual experiments, the catalyst is kept at 673 K in 3 : 1 H₂ : N₂ to avoid deactivation of the catalyst by oxygen adsorption. To obtain a catalyst surface free of contaminants from the gas phase, the following procedure is adopted prior to an adsorption experiment: the activity of the catalyst is checked at 673 K. The temperature is increased to 823 K and the flow switched to H₂.

After a minimum of 30 min, the NH_3 and N_2 levels are identical whether the reactor is bypassed or not, and in order to free the surface from hydrogen, He is passed over the catalyst for a minimum of 45 min. Then the catalyst is cooled to the adsorption temperature. Adsorption experiments are performed with a He gas containing 0.10% N_2 and the adsorption rate is followed as a function of time by measuring the N_2 content in the gas after it passes the catalyst bed. This is done with a mass spectrometer where the N_2 signal is calibrated just before and after an adsorption experiment. Passing the N_2 gas over the uncovered catalyst starts the adsorption experiment. The starting time of the experiment is corrected for the time it takes the gas to replace the He in the reactor (the dead volume). The correction time amounted to 8 ± 2 s at a flow rate of 6.0 L/h (STP). Continuing the H_2 and He flush for longer than 30 and 45 min, respectively, was not necessary since this had no influence on the results.

Temperature-programmed nitrogen desorption is carried out with the catalyst saturated with nitrogen. In a flow of pure He, the temperature is raised to 823 K at 480 K/h while the N_2 content of the exit gas is determined. No gases other than N_2 were detected during the desorption experiment. Electronic mass flow controllers control the flow of each gas line. All gases used in the activity measurements and dinitrogen dissociation experiments are of 99.9999% purity and are purified further by flowing them over a large volume of KM1R catalyst kept at room temperature. This guard is regenerated at regular intervals.

RESULTS AND DISCUSSION

The ammonia synthesis activity of the cesium-promoted $\text{Co}_3\text{Mo}_3\text{N}$ catalyst at 713, 673, 633, and 593 K, and a total pressure of 10 bar in a 3 : 1 mixture of dihydrogen and dinitrogen, is shown in Fig. 1. The activity of $\text{Cs}/\text{Co}_3\text{Mo}_3\text{N}$ is slightly lower than that previously reported, but still higher than that of the industrial multipromoted iron catalyst, KM1 (21). It is interesting that the activity of $\text{Cs}/\text{Co}_3\text{Mo}_3\text{N}$ (a) is about three times lower than that of $\text{Cs}/\text{Co}_3\text{Mo}_3\text{N}$, reflecting the differences in crystal sizes. In our experiments with these catalysts, the general observation was that the preparation route and pretreatment condition could influence the activity significantly. In this context it should be noted that Kojima and Aika have also observed that the activity can be increased by passivation followed by reactivation (32). These observations could indicate that ammonia synthesis is a structure-sensitive reaction over $\text{Co}_3\text{Mo}_3\text{N}$, as is also the case with other catalysts (28, 33–36). The activity of $\text{Cs}/\text{Co}_3\text{Mo}_3\text{N}$ is seen to be between 6 and $2.3 \mu\text{mol g}^{-1} \text{s}^{-1}$ at 673 K and 10 bar in 3 : 1 H_2 : N_2 (dependent on the ammonia concentration). At similar conditions, Kojima and Aika report an activity of ca. $2.2 \mu\text{mol g}^{-1} \text{s}^{-1}$ for a $\text{Cs}/\text{Co}_3\text{Mo}_3\text{N}$ catalyst with a surface area of about $35 \text{ m}^2/\text{g}$ but the am-

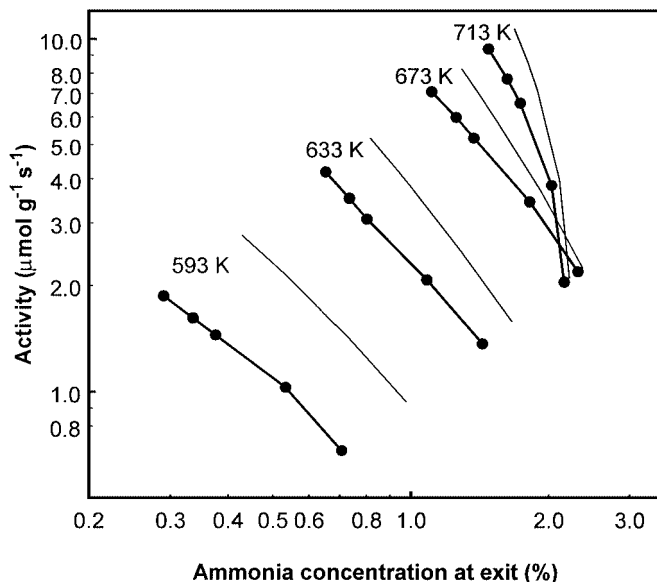


FIG. 1. Activity of cesium-promoted $\text{Co}_3\text{Mo}_3\text{N}$ measured at 713, 673, 633, and 593 K. Catalyst (0.3036 g), 10 bar total pressure, H_2 : N_2 = 3 : 1, and, 2.4–16 L/h total flow at STP were used. Catalytic activities determined from the microkinetic model are given for comparison. At these conditions, the microkinetic model slightly overestimates the activity but generally the agreement between the measurements and the model is excellent.

monia concentration is not specified and therefore a direct comparison is not possible. Recently, power-law kinetics were developed for $\text{Cs}/\text{Co}_3\text{Mo}_3\text{N}$ from activity measurements obtained at 1 bar (24). However, from Fig. 1 it can be seen that the slopes of the curves (which are measures of the ammonia reaction orders) are dependent on pressure, temperature, and gas composition. This suggests, as is usually found for ammonia synthesis catalysts, that it is not possible to give an accurate description of the reaction kinetics with a power-law expression. Furthermore, power-law kinetics have been shown only to be accurate far from equilibrium in ammonia synthesis (37). From an industrial perspective, it is much more relevant to establish the reaction kinetics at conditions close to equilibrium. Therefore, we decided to construct a microkinetic model since this would also enable more detailed insight into the role of Co and Mo in the catalyst. As a first step it is necessary to determine the total number of surface sites. This is usually done by nitrogen TPD. Therefore, the number of surface sites on the cesium-promoted $\text{Co}_3\text{Mo}_3\text{N}$ catalyst capable of binding nitrogen was determined by a temperature-programmed desorption experiment, as shown in Fig. 2. Desorption of nitrogen from the catalyst surface starts at approximately 518 K. The onset of the second peak at 718 K is attributed to the loss of bulk nitrogen from the ternary nitride catalyst material. Attributing only the first peak to loss of surface nitrogen results in the number of sites capable of binding nitrogen, which is $30 \mu\text{mol}/\text{g}$. This is comparable to KM1 (38), which has a comparable surface area. Traditionally, dissociative

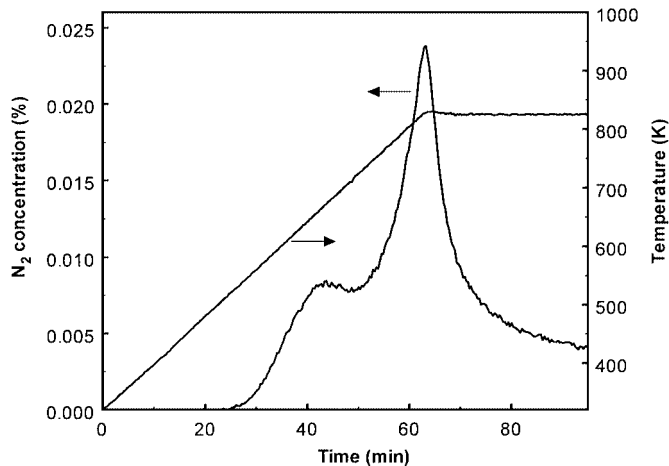
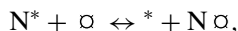


FIG. 2. TPD after N_2 adsorption. The heating rate was 480 K/h and He flow 6.00 L/h at STP. The N_2 desorption peak corresponds to $30 \mu\text{mol/g}$. The second peak is attributed to loss of bulk nitrogen beginning at 718 K.

adsorption of dinitrogen on ammonia synthesis catalysts has been described by a Freundlich isotherm (39, 40) and this is the reason that the Temkin–Pyzhev equation (41) was introduced to describe the ammonia synthesis kinetics of industrial reactors. We have recently shown that it is possible to give an alternative interpretation of the adsorption experiment described. Accordingly, the N_2 adsorption on KM1 was accurately described using a Langmuirian model assuming that only a fraction of the sites on the catalyst surface is able to dissociate N_2 , and that the remaining sites are filled with N through surface diffusion from the active sites. Due to fast surface diffusion of N on Fe (42) it was assumed that the N adsorbed on the active sites is in equilibrium with the N adsorbed on the inactive sites,



where * and \square denote active and inactive sites, respectively. We decided to elucidate the N_2 adsorption on Cs/ $\text{Co}_3\text{Mo}_3\text{N}$ through isothermal experiments. The isothermal N_2 adsorption was measured at 500, 550, 600, 650, and 700 K. Figure 3 shows the result of such an experiment performed at 500, 550, and 600 K. It is seen that initially the catalyst adsorbs all the N_2 in the gas feed. After a short period, the amount of N_2 passing the catalyst without being adsorbed increases rapidly and finally reaches a level where only a small amount of N_2 is being adsorbed. After 1 h, the catalyst was not completely saturated with nitrogen. Similar adsorption isotherms were obtained at the other temperatures and it was generally not possible to model the adsorption isotherms with a single-site Langmuirian model. However, using the previously reported procedure (31) summarized above, we were able to accurately describe the N_2 adsorption isotherms also on Cs/ $\text{Co}_3\text{Mo}_3\text{N}$, as shown in Fig. 3. It was possible to achieve a satisfactory agreement between

experiments and the model by using a ratio of active and inactive sites between ca. 0.5 and 5%. The choice of the relative number of active sites only influences the equilibrium constant that relates the coverages of the active and inactive sites. We have chosen to assume that 1% of the surface sites is active for N_2 dissociation and this results in an equilibrium constant similar to that found on the multipromoted iron catalyst (31). Satisfactory agreement between experiment and model is achieved at all temperatures except at 700 K, where the amount of N_2 adsorbed is higher than expected from the model. This is ascribed to diffusion of N_2 into the bulk of the catalyst at high temperatures. This explanation is consistent with the TPD experiment that showed loss of nitrogen from the bulk above 718 K. In Fig. 4, the resulting initial sticking coefficients are shown in an Arrhenius form. The temperature dependency is adequately described by $s_0 = 0.1727 \cdot \exp((-42.8 \pm 5 \text{ kJ/mol})/RT)$. This activation energy for dinitrogen dissociation is close to the one found on Ru and therefore clearly between that of Co and of Mo, as is proposed by the interpolation principle and calculated using DFT (30). Thus, the presence of mixed Co–Mo surface sites in the structure is required in order to explain the result. The (111) surface of $\text{Co}_3\text{Mo}_3\text{N}$ clearly exposes such mixed sites (30) according to the structure determination by Alchonel (43). Using the kinetics for dinitrogen dissociation and the number of active sites resulting from the isothermal N_2 adsorption experiments, we have constructed a Langmuir–Hinshelwood-type microkinetic model taking the following reactions into account:

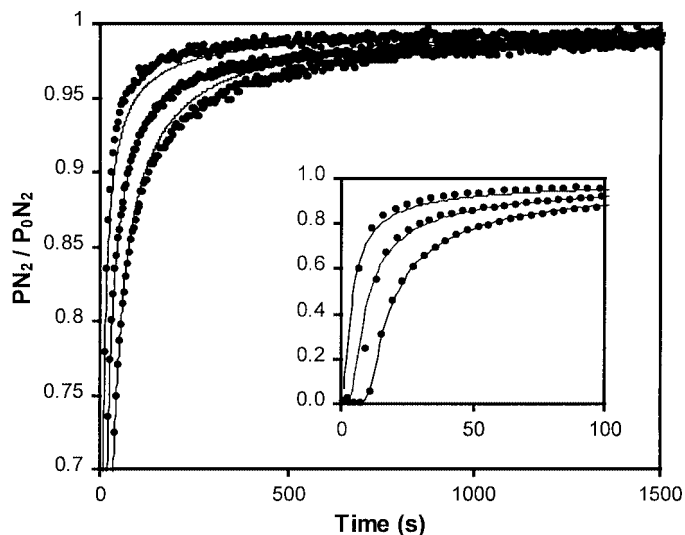


FIG. 3. N_2 adsorption on cesium-promoted $\text{Co}_3\text{Mo}_3\text{N}$ at 500, 550, and 600 K using a gas flow of 6.00 L/h at STP. The experimental results are depicted as dots while the prediction of the model discussed in the text is depicted as a full line.

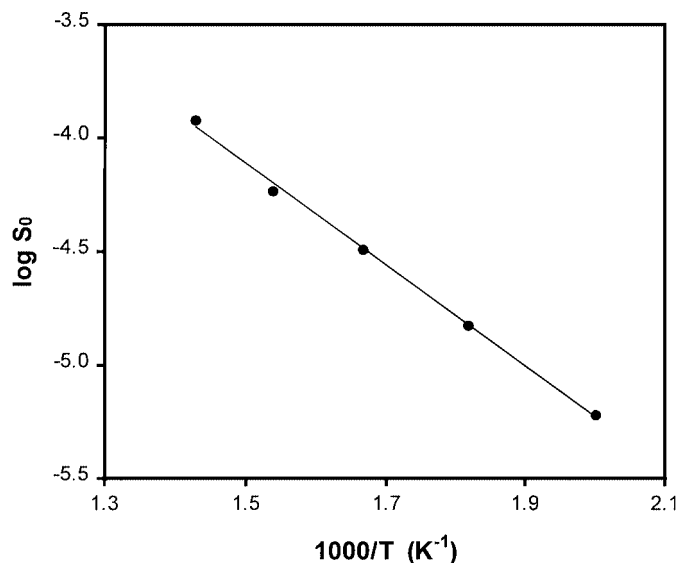
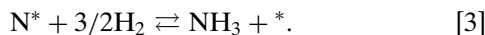


FIG. 4. Initial sticking coefficients of N_2 on the active sites obtained by fitting the model discussed in the text to the experimental results.



Reaction [1] is the rate-limiting step and reactions [2] and [3] are assumed to be in equilibrium. Assuming an area per active site of 10^{-19} m^2 , the rate constant per active site for nitrogen dissociation is determined from s_0 as $k_1 = 4.98 \times 10^9 \cdot s_0 \cdot T^{-0.5} \text{ K}^{0.5} \text{ bar}^{-1} \text{ s}^{-1}$. It is known that the hydrogen-binding energy changes only slightly on different transition metals compared to the nitrogen-binding

energy. Therefore, we have used an equilibrium constant of $2.14 \times 10^{-7} \text{ bar}^{-1} \exp(96.0 \text{ kJ/mol/RT})$ for reaction [2], as was also been done in a recent microkinetic model for ammonia synthesis over KM1 (44). The starting value for the equilibrium constant of reaction [3] is also taken from the microkinetic model describing KM1 and only the reaction enthalpy was changed in order to fit the model to the Cs/ Co_3Mo_3N activity data. Thus, the preexponential factors we use in the model for reactions [2] and [3] are equal to the ones used to describe ammonia synthesis over an iron catalyst. These values are close to the values obtained by statistical mechanics analysis of the reactions over ruthenium (45) and it is therefore assumed that they can also be used to describe the reaction over Co_3Mo_3N .

As shown in Fig. 5, an excellent agreement can be achieved with an equilibrium constant of $37.0 \text{ bar}^{-1/2} \exp(-31.5 \text{ kJ/mol/RT})$ for reaction [3]. This corresponds to a reaction enthalpy for nitrogen adsorption [1] of -154.8 kJ/mol . This nitrogen-binding energy on the active sites of Co_3Mo_3N is very close to the binding energy found on the active Fe sites on KM1 (31) and therefore between that of molybdenum and cobalt (30). This shows that a microkinetic model consistent with the TPD, the isothermal adsorption, the activity measurements covering a wide range of experimental conditions, and the interpolation principle has been developed. The same model can also be used to describe the activity of the Cs/ Co_3Mo_3N (a) catalyst only by reducing the number of active sites to $1/3$. Since the activities of Cs/ Co_3Mo_3N and Cs/ Co_3Mo_3N (a) are very different, this is a strong indication that the model captures the important characteristics of the active sites on the ternary nitride catalyst. However, it is now well

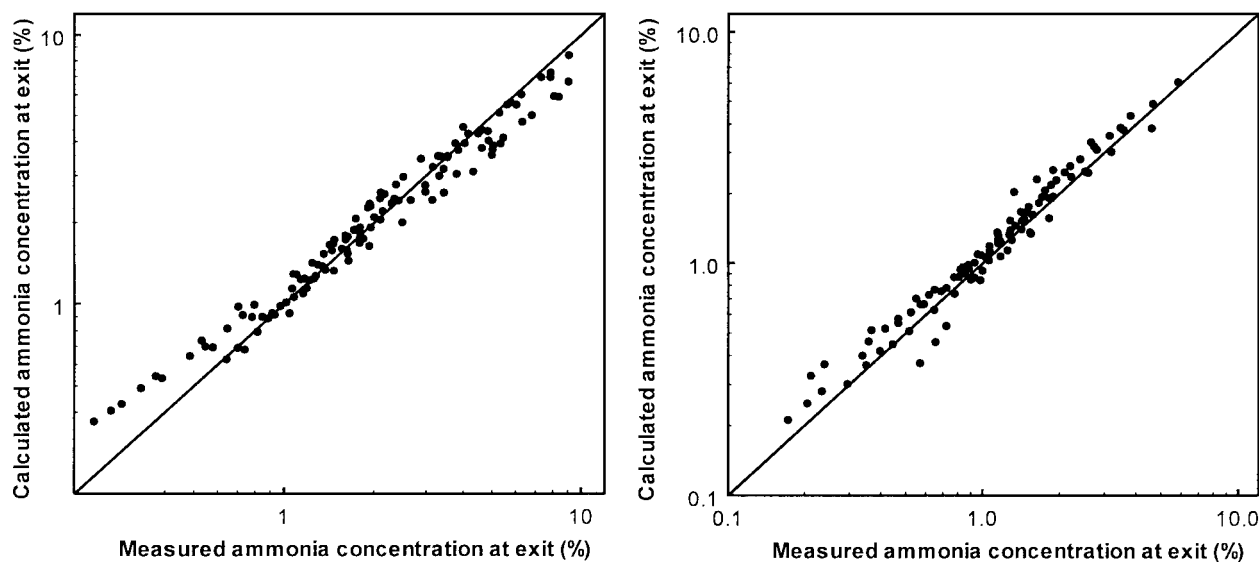


FIG. 5. Ammonia concentrations predicted by the model discussed in the text plotted as a function of the measured ammonia concentrations for Cs/ Co_3Mo_3N (left) and Cs/ Co_3Mo_3N (a) (right), with $H_2:N_2$ ratios of 3:1 and 1:1; total pressures of 50, 25, and 10 bar; and temperatures from 593 to 713 K.

documented that microkinetic models with very different parameters can be used to describe even extensive catalytic activity measurements obtained with the same catalyst (44, 46–49). Particularly, very different kinetic models have been shown to give reasonable agreement with the available activity measurements with the multipromoted iron catalyst for ammonia synthesis. It is noteworthy that in our present approach, we derive a set of consistent kinetic parameters from catalyst studies. We show that it is necessary to clearly distinguish between inactive sites and active sites in order to accurately model both the steady-state catalytic activities and at the same time the non-steady-state desorption experiments. It would be interesting to verify these parameters, e.g., through single-crystal studies. Therefore, we attempted to evaporate Co onto a surface-nitrided Mo(111) surface in the UHV setup previously described (50). The ammonia synthesis activity of the surfaces was measured at 2 bar. Although it was clear that Co was a promoter for the nitrided Mo surface resulting in a significantly increased (three times as high) ammonia production, it was not possible to obtain reliable steady-state measurements since Co diffused from the surface of the nitrided Mo crystal to the bulk at the temperatures studied (673–873 K). Although the kinetic model derived above gives a very accurate description of the activity measurements and is in excellent agreement with the DFT calculations, it should be noted that this might be an oversimplification. It is above all not certain that the site(s) active for ammonia synthesis during the catalytic activity measurements are the same sites as those primarily responsible for dinitrogen dissociation during the isothermal adsorption experiment. In practice, different sites with different ratios of Co to Mo atoms could be exposed at the catalyst surface. More detailed insight into the surface structure of the active catalyst during reaction conditions is necessary to clarify this aspect. However, it appears that the interpolation concept can be used to rationalize the activity of the Cs/Co₃Mo₃N catalyst. Thus, the effect of cesium is similar to that observed by alkali promotion of other transition-metal-based ammonia synthesis catalysts, i.e., promotion occurs through an electrostatic effect (29). The success of this simple model suggests that other ammonia synthesis catalysts could be designed using the same approach, that is, by combining metals from both sides of the volcano curve. This approach could possibly also be used to design catalyst for other reactions, as recently suggested (51).

REFERENCES

- Oyama, S. T., Ed., "The Chemistry of Transition Metal Carbides and Nitrides" Blackie Academic, Glasgow, 1996.
- Levy, R. B., and Boudart, M., *Science* **181**, 547 (1973).
- Leclercq, L., in "Surface Properties and Catalysis by Nonmetals" (J. P. Bonelle, B. Delmon, and E. Derouane, Eds.), p. 433. Reidel, Dordrecht, 1983.
- Claridge, J. B., York, A. P. E., Brungs, A. J., and Green, M. L. H., *Chem. Mater.* **12**, 132 (2000).
- Boudart, M., Oyama, S. T., and Volpe, L., U.S. Patent 4,515,763 (1985).
- Lee, J. S., and Boudart, M., *Appl. Catal.* **19**, 207 (1983).
- Markel, E. J., and Van Zee, J. W., *J. Catal.* **126**, 643 (1990).
- Nagai, M., and Miyao, T., *Catal. Lett.* **18**, 9 (1993).
- Claridge, J. B., York, A. P. E., Brungs, A. J., Márquez-Alvarez, C., Sloan, J., Tsang, S. C., and Green, M. L. H., *J. Catal.* **180**, 85 (1998).
- York, A. P. E., Claridge, J. B., Márquez-Alvarez, C., Brungs, A. J., Tsang, S. C., and Green, M. L. H., *Stud. Surf. Sci. Catal.* **110**, 711 (1997).
- Patt, J., Moon, D. J., Phillips, C., and Thompson, L., *Catal. Lett.* **65**, 193 (2000).
- Oyama, S. T., *Catal. Today* **15**, 179 (1992).
- Liang, C., Li, W., Wei, Z., Xin, Q., and Li, C., *Ind. Eng. Chem. Res.* **39**, 3694 (2000).
- Ribeiro, F. H., Boudart, M., Dalla Betta, R. A., and Iglesia, E., *J. Catal.* **130**, 498 (1991).
- Kojima, I., Miyazaki, E., Inoue, Y., and Yasumori, I., *J. Catal.* **73**, 128 (1982).
- Boudart, M., Locatelli, S., Lee, J. S., and Oyama, S. T., *J. Catal.* **125**, 157 (1990).
- Sehested, J., Jacobsen, C. J. H., and Rostrup-Nielsen, J. R., *J. Catal.* **201**, 206 (2001).
- Wang, L. T., Xie, M., Xu, G., Huang, J., and Xu, Y., *Catal. Lett.* **21**, 35 (1993).
- Hamid, S. B. D.-A., Anderson, J. R., Schmidt, I., Bouchy, C., Jacobsen, C. J. H., and Derouane, E. G., *Catal. Today* **63**, 461 (2000).
- Jacobsen, C. J. H., Brorson, M., Sehested, J., Teunissen, H., and Törnqvist, E., U.S. Patent 6,235,676 (1999) to Haldor Topsøe A/S.
- Jacobsen, C. J. H., *Chem. Commun.* 1057 (2000).
- Kojima, R., and Aika, K., *Chem. Lett.* 514 (2000).
- Kojima, R., and Aika, K., *Appl. Catal. A* **215**, 149 (2001).
- Kojima, R., and Aika, K., *Appl. Catal. A* **218**, 121 (2001).
- Patt, J., Bej, S., and Thompson, L., in "Proc. 17th North American Catalysis Society Meeting, Toronto 2001," p. 70.
- Dadyburjor, D. B., Iyer, M. V., Kugler, E. I., and Norcio, L., in "Proc. 17th North American Catalysis Society Meeting, Toronto 2001," p. 104.
- Schlögl, R., in "Handbook of Heterogeneous Catalysis" (G. Ertl, H. Knözinger, and J. Weitkamp, Eds.), p. 1697. Wiley-VCH, Weinheim, 1997.
- Logadottir, A., Rod, T. H., Nørskov, J. K., Hammer, B., Dahl, S., and Jacobsen, C. J. H., *J. Catal.* **197**, 229 (2001).
- Dahl, S., Logadottir, A., Jacobsen, C. J. H., and Nørskov, J. K., *Appl. Catal. A*, **222**, 19 (2001).
- Jacobsen, C. J. H., Dahl, S., Clausen, B. S., Bahn, S., Logadottir, A., and Nørskov, J. K., *J. Am. Chem. Soc.* **123**, 8404 (2001).
- Dahl, S., Törnqvist, E., and Jacobsen, C. J. H., *J. Catal.* **198**, 97 (2000).
- Kojima, R., and Aika, K., *Appl. Catal.* **219**, 157 (2001).
- Ertl, G., in "Catalytic Ammonia Synthesis: Fundamentals and Practice" (J. R. Jennings, Ed.), p. 109. Plenum, New York, 1991.
- Strongin, D. R., and Somorjai, G. A., in "Catalytic Ammonia Synthesis: Fundamentals and Practice" (J. R. Jennings, Ed.), Ch. 1. p. 133. Plenum, New York, 1991.
- Tennison, S. R., in "Catalytic Ammonia Synthesis: Fundamentals and Practice" (J. R. Jennings, Ed.), p. 303. Plenum, New York, 1991.
- Dumesic, J. A., Topsøe, H., Khammouma, S., and Boudart, M., *J. Catal.* **37**, 503 (1975).
- Holzman, P. R., Shiflett, W. K., and Dumesic, J., *J. Catal.* **62**, 167 (1980).
- Fastrup, B., *J. Catal.* **150**, 345 (1994).
- Emmett, P. H., and Brunauer, S., *J. Am. Chem. Soc.* **56**, 35 (1934).
- Scholten, J. J. F., Zwiering, P., Konvalinka, J. A., and de Boer, H. J., *Trans. Faraday Soc.* **55**, 2166 (1959).

41. Temkin, M., and Pyzhev, V., *Acta Physicochim. USSR* **12**, 327 (1940).
42. Pedersen, M. Ø., Österlund, L., Mortensen, J. J., Mavrikakis, M., Hansen, L. B., Steensgaard, I., Lægsgaard, E., Nørskov, J. K., and Besenbacher, F., *Phys. Rev. Lett.* **84**, 4898 (2000).
43. Alchonel, S., *J. Mater. Chem.* **8**, 1901 (1998).
44. Sehested, J., Jacobsen, C. J. H., Törnqvist, E., Rokni, S., and Stoltze, P., *J. Catal.* **188**, 83 (1999).
45. Dahl, S., Sehested, J., Jacobsen, C. J. H., Törnqvist, E., and Chorkendorff, I., *J. Catal.* **192**, 391 (2000).
46. Bowker, M., Parker, I. B., and Waugh, K. C., *Appl. Catal.* **14**, 101 (1985).
47. Stoltze, P., and Nørskov, J. K., *Phys. Rev. Lett.* **55**, 2502 (1985).
48. Fastrup, B., *Top. Catal.* **1**, 273 (1994).
49. Dumesic, J. A., and Trevino, A. A., *J. Catal.* **116**, 119 (1989).
50. Törnqvist, E., and Chen, A. A., *Catal. Lett.* **8**, 359 (1991).
51. Nørskov, J. K., Bligaard, T., Logadottir, A., Bahn, S., Hansen, L. B., Bollinger, M., Bengaard, H., Hammer, B., Sljivancanin, Z., Mavrikakis, M., Xu, Y., Dahl, S., and Jacobsen, C. J. H., *J. Catal.*, accepted for publication.